Central European Journal of Energetic Materials
ISSN 1733-7178; e-ISSN 2353-1843

Cent. Eur. J. Energ. Mater. 2017, *14*(4): 876-887; DOI: 10.22211/cejem/77125

Preparation and Characterization of Ultrafine HMX/TATB Explosive Co-crystals

Chongwei An,[1*] Hequn Li,[1] Yuruo Zhang,[2] Baoyun Ye,[1] Chuanhao Xu,[1] Jingyu Wang [1]**

[1] School of Environment and Safety Engineering/Shanxi Engineering Technology Research Center for Ultrafine Powder, North University of China, Xueyuan Road No. 3, 030051 Shanxi Taiyuan, China
[2] The 213th Research Institute of China Ordnance Industry, Xi'an 710061, Shaanxi, China
*E-mails: *anchongwei@yeah.net; **lhq6371630@163.com*

Abstract: An explosive co-crystal of 1,3,5,7-tetranitro-1,3,5,7-tetraazacyclooctane (HMX) and 1,3,5-triamino-2,4,6-trinitrobenzene (TATB) was prepared by the ball milling method. The raw materials and co-crystals were characterized using scanning electron microscopy (SEM), X-ray diffraction (XRD), differential scanning calorimetry (DSC) and Raman spectroscopy. Impact and friction sensitivity of the co-crystals were tested and analyzed. The results showed that the HMX/TATB co-crystals are spherical in shape and 100-300 nm in size. The co-crystals are different from anintimate mixture of HMX/TATB and they exhibit a new co-crystal structure. HMX/TATB co-crystals are formed by N-O···H hydrogen bonding between $-NO_2$ (HMX) and $-NH_2$ (TATB). The drop height of ultrafine HMX/TATB explosive co-crystals is 12.7 cm higher than that of ultrafine HMX, whilst the explosion probability of friction is 20% lower than that of ultrafine HMX. Ultrafine HMX/TATB explosive co-crystals are difficult to initiate under impact and friction conditions.

Keywords: HMX, TATB, ultrafine co-crystals, ball milling, mechanical sensitivity

1 Introduction

In recent years, co-crystal technology has attracted extensive attention of energetic materials researchers who have applied it in the modification of energetic materials [1]. Co-crystal explosives, with good comprehensive properties, based on CL-20 [2-4], HMX [5-7], TNT [8], BTF [9, 10] and NTO [11] have been synthesized.

HMX has been generally used as the main ingredient in munitions and propellants due to its high energy output and destructibility. However, its high mechanical sensitivity restricts its actual military application. TATB favours the preparation of insensitive munitions because of its moderate power, low mechanical sensitivity and high heat-resistant property. It was of interest to verify whether or not co-crystal technology could combine the brilliant properties of HMX and TATB. Therefore, continued study of HMX/TATB explosive co-crystals has been conducted by the researchers at the Southwest University of Science and Technology (China) and the Chinese Academy of Engineering Physics. Initially, the equilibrium structures of different HMX/TATB co-crystal models were simulated through molecular dynamics. The co-crystal structure of HMX/TATB was most stable when the HMX molecule was substituted by TATB on the surface of the HMX crystal, with the lowest surface free energy and the slowest growth rate [12]. Subsequently, the HMX/TATB co-crystal structure was predicted using the polymorph predictor method. It belonged to the $P\bar{1}$, $P2_12_12_1$ or $P2_1/c$ space group. The mechanical properties, stability and intermolecular interaction energy of the HMX/TATB co-crystals were simulated through molecular dynamics. The mechanical properties and stability of the co-crystals were improved because the moduli systematically decreased and the trigger bond $N{-}NO_2$ was modified. This phenomenon can be explained by the presence of strong van der Waals interactions and hydrogen bonds between the HMX and TATB molecules [13]. On the basis of previous studies, HMX/TATB explosive co-crystals were prepared using the solvent/nonsolvent method. The co-crystals formed presented polyhedral shapes and their particle sizes were approximately 20-30 μm [14]. In terms of reducing the mechanical sensitivity [15-17] and improving the reaction rate [18-20], ultrafine explosive particles have an advantage over large ones. Thus far, ultrafine CL-20/HMX and CL-20/TNT explosive co-crystals have been prepared through the spray flash evaporation process [21, 22], whereas nano CL-20/HMX co-crystals have been synthesized through the ultrasonic spray-assisted electrostatic adsorption method [23]. Ultrafine CL-20/TNT and nano HMX/TNT co-crystals with low sensitivity were prepared in our previous studies by the spray drying method [24, 25]. In the three preparative methods mentioned above, it is necessary to select a suitable

solvent to dissolve the entire explosive. However, TATB has low solubility in traditional solvents including dimethyl sulfoxide (DMSO). Therefore, these spray methods are not appropriate for preparing explosive co-crystals with TATB inclusions. Mechanical milling is a green environmentally-friendly preparative method without the use of organic solvents and is an unusually significant method for preparing pharmaceutical co-crystals [26, 27] and ultrafine explosives [28]. Qiu *et al*. first adopted a bead milling method to prepare nanoscale CL-20/HMX co-crystal particles [29].

On the basis of previous studies of HMX/TATB explosive co-crystals, ultrafine HMX/TATB (molar ratio 8/1) explosive co-crystals were prepared by the ball milling method. Furthermore, the morphology, size, X-ray diffraction, thermolysis, reasons for co-crystal formation, impact sensitivity and friction sensitivity of the ultrafine co-crystals were investigated in detail.

2 Experimental Section

2.1 Materials

HMX and TATB were provided by Gansu Yinguang Chemical Industry Co. Ltd. of China. Deionized water was laboratory prepared. The YXQN type planet type ball mill and zirconia balls (0.1 mm) were purchased from Changsha Miqi Instrument Equipment Co. Ltd. of China. The KQ-300E ultrasonic cleaner was purchased from Kunshan Ultrasonic Instruments Co. Ltd. of China.

2.2 Sample preparation

Firstly, HMX (9.02 g), TATB (0.98 g), deinonized water (100 mL) and zirconia balls (200 g) were added to the ceramic ball mill pot. Then, the planet type ball mill was used to produce the explosive co-crystals. The revolution and rotation speed were 300 r/min and 600 r/min, respectively. The milling time was set to 8 h.

The operating principle of the planet type ball mill is that four ball mill pots on the circumference of the rotating disk rotate along with the wheel revolution and high-speed rotation. Under this circumstance, the milling balls and material particles in the mill pots will go through the process of collision, shearing and friction, which resulted in the object of smash, grind, mixing and reaction.

Finally, the white zirconia balls and yellow suspension were separated using sonication. After filtration, washing, and freeze drying of the yellow suspension, the objective sample was obtained.

Ultrafine HMX (10 g) and ultrafine TATB (10 g) were prepared as reference samples using the same process.

2.3 Characterization of samples

A Mira3 LMH scanning electron microscope, which was manufactured by TESCAN of the Czech Republic, was used to characterize the particle size and morphology of the samples.

An X-ray diffractometer, which was made by Dandong Haoyuan Instrument Co. Ltd. of China, was used to identify HMX, TATB and the prepared co-crystal sample. The testing conditions included the target material (Cu) with a tube voltage of 40 kV, tube current of 30 mA, a start angle of 5°, and an end angle of 50°.

Differential scanning calorimetry was carried out using a Setaram DSC 131 instrument from France. In the test, each sample (0.7 mg) was placed in a closed aluminum crucible of 30 μL volume with a hole in the lid. The samples were measured with a temperature profile of 40 °C to 420 °C at a heating rate of 10 K/min in a nitrogen atmosphere, flow rate 30 mL/min.

A Raman spectroscopy instrument, manufactured by Bio-Rad Co. Ltd., USA, was used to explore the reasons for the formation of co-crystals. Raman excitation light provided by a 532 nm beam from an argonion laser and 0.5 mW power was used for all measurements. For each sample, the spectrum was obtained by averaging 20 scans with a measurement time of 5 s per scan.

An ERL type 12-drop hammer apparatus was used to conduct the impact sensitivity tests according to the GJB-772A-97 standard method 601.3 [30]. The testing conditions consisted of a drop weight of 2.500 ±0.002 kg, a sample mass of 35 ±1 mg and a relative humidity of 50%. The critical drop-height of 50% explosion probability (H_{50}) was used to represent the test results.

A WM-1 pendulum friction apparatus was used to test the friction sensitivity based on the GJB-772A-97 standard method 602.1 [30]. The experimental conditions were as follows. Pendulum weight, 1.5 kg; swing angle 90°; pressure 3.92 MPa; sample mass 20 ±1 mg and test number 25. Friction sensitivity was expressed as explosion probability (P).

3 Results and Discussion

3.1 SEM

Figure 1 shows the SEM images of the raw HMX, the raw TATB, an ultrafine HMX/TATB mixture with a molar ratio of 8/1 and the HMX/TATB co-crystals. The morphology of the raw HMX particles was of a polyhedral shape with an uneven size distribution and an average particle size of ca. 100 μm. The raw TATB particles had extremely rough surfaces with many edges and corners. The

particle size of the raw TATB was ca. 5-20 μm. No significant difference was observed between the particle size and morphology of the ultrafine HMX/TATB mixture and the HMX/TATB co-crystals. They were spherical in shape and ranged from 100 nm to 300 nm.

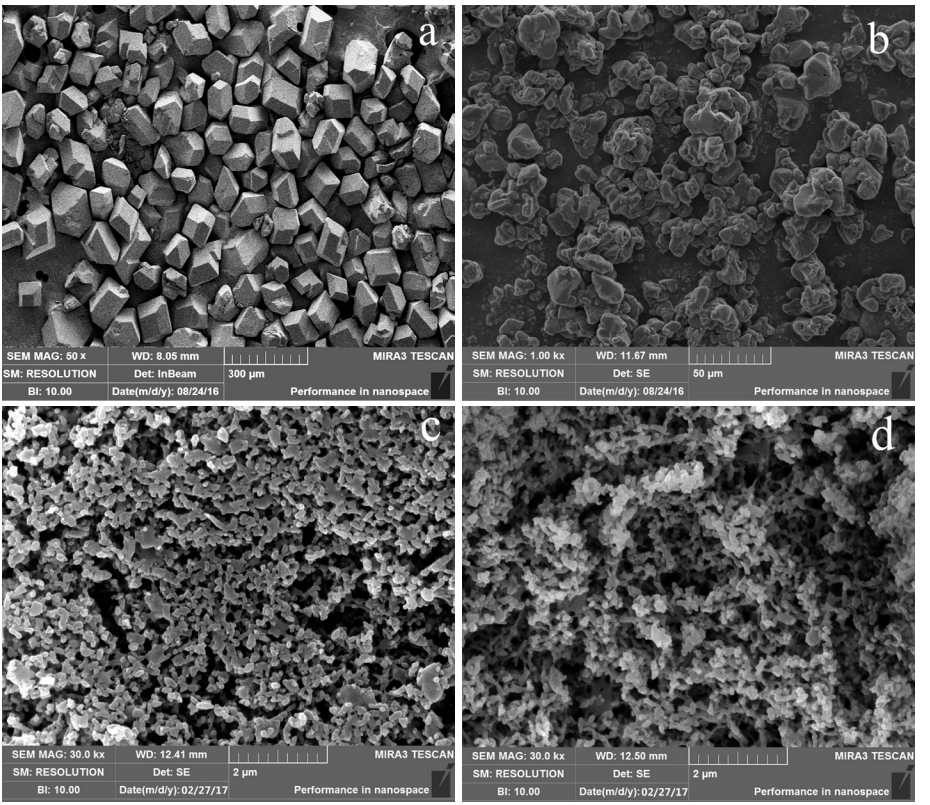

Figure 1. SEM images of (a) raw HMX, (b) raw TATB, (c) ultrafine HMX/TATB mixture with a molar ratio of 8/1, and (d) HMX/TATB co-crystals

3.2 XRD

Raw HMX, raw TATB, and HMX/TATB co-crystals were examined by X-ray diffraction. The observed patterns are shown in Figure 2. The crystal form of raw HMX was identified as the β-type using MDI Jade 9 and PDF 2009 software. In Figure 2 all the diffraction peaks of raw HMX appear in the pattern of the HMX/TATB co-crystals. However, only the diffraction peak of raw TATB at 28.4° appears in that pattern. The result showed that the explosive sample,

which was prepared by the ball milling method, was not simply mixed, but that HMX and TATB had interacted to form a new co-crystal structure. In addition, the peaks of the explosive co-crystals were much weaker and wider than those of the raw samples. This phenomenon was caused by X-ray dispersion, which was induced by the small co-crystal particles. This is confirmed by the result presented in Figure 1c.

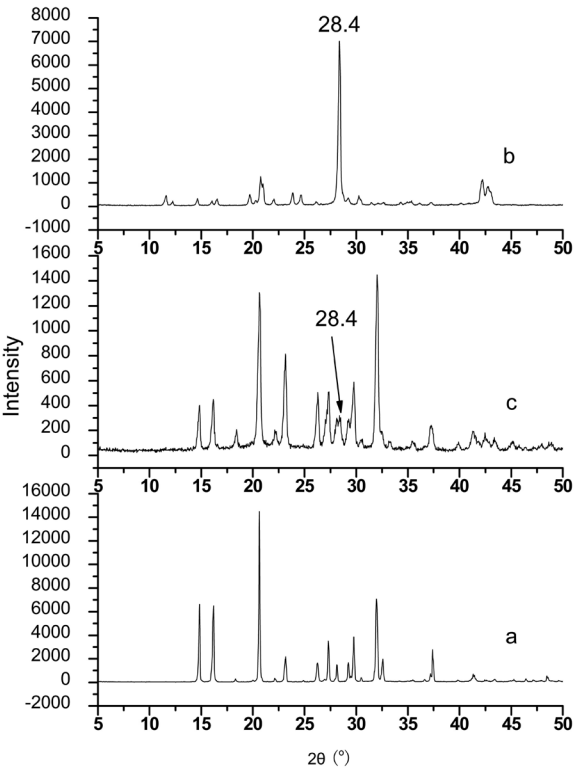

Figure 2. XRD patterns of (a) raw HMX, (b) raw TATB, and (c) HMX/TATB co-crystals

3.3 DSC

Figure 3 shows the DSC curves of raw HMX, raw TATB, a mixture of raw HMX/TATB with a molar ratio of 8/1, an ultrafine HMX/TATB mixture with a molar ratio of 8/1, and the HMX/TATB co-crystals at a heating rate of 10 K/min. It shows that the melting endothermic peaks of the raw HMX and the raw HMX/TATB mixture and ultrafine HMX/TATB mixture are obvious at approximately 280 °C. However, this phenomenon does not occur in the co-

crystal sample. Comparing the DSC curves of the two mixtures, the temperatures of the two exothermic peaks and the single endothermic peak from the ultrafine mixture are approximately 4 °C lower than those of the raw mixture. Compared with the DSC curves of the raw and ultrafine HMX/TATB mixture, the exothermic peak temperature of TATB in the curve of the co-crystals does not appear around 380 °C. Thus, the changes reveal that the HMX/TATB co-crystals are not an intimate mixture of HMX/TATB and exhibit thermal stability that is indistinguishable from that of HMX.

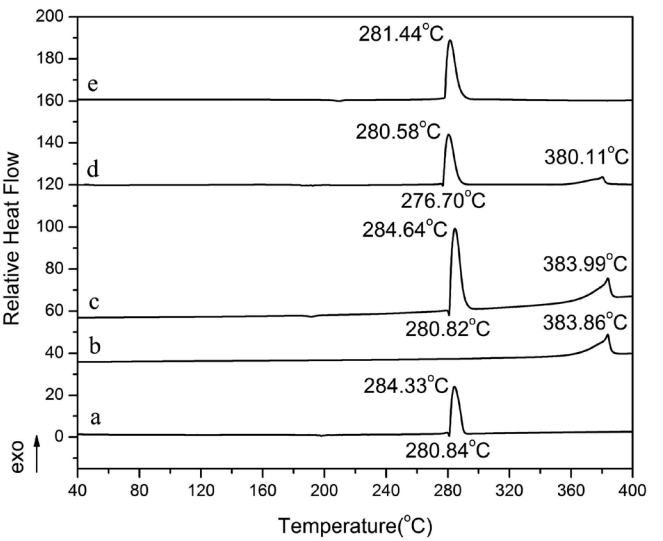

Figure 3. DSC curves of (a) raw HMX, (b) raw TATB, (c) raw HMX/TATB mixture with a molar ratio of 8/1, (d) ultrafine HMX/TATB mixture with a molar ratio of 8/1, and (e) HMX/TATB co-crystals at a heating rate of 10 K/min

3.4 Raman spectroscopy

The Raman spectra of raw HMX, raw TATB and HMX/TATB co-crystals are presented in Figure 4. The assignments of the major bands of the Raman spectra of the samples are listed in Table 1. Figure 4 and Table 1 show that several HMX and TATB peaks shift markedly in the Raman spectrum of the co-crystals. In TATB, the $-NH_2$ stretch shifts from 3223.7 cm^{-1} to 3214.0 cm^{-1}. The C-N stretch shifts from 1609.0 cm^{-1} to 1603.4 cm^{-1} in the $C-NO_2$ group, and the peak which represents the asymmetric $-CH_2-$ stretch vibration in HMX, shifts from 2991.7 cm^{-1} to 2993.0 cm^{-1}. The asymmetric $-NO_2$ stretch vibration shifts from 1556.2 cm^{-1} to 1565.9 cm^{-1} in the $-NO_2$ group of HMX. These changes can be

attributed to the N−O···H hydrogen bonding between $-NH_2$ (TATB) and $-NO_2$ (TATB), which is destroyed by mechanical action. Moreover, it contributes to the formation of the N−O···H hydrogen bonding between $-NO_2$ (HMX) and $-NH_2$ (TATB).

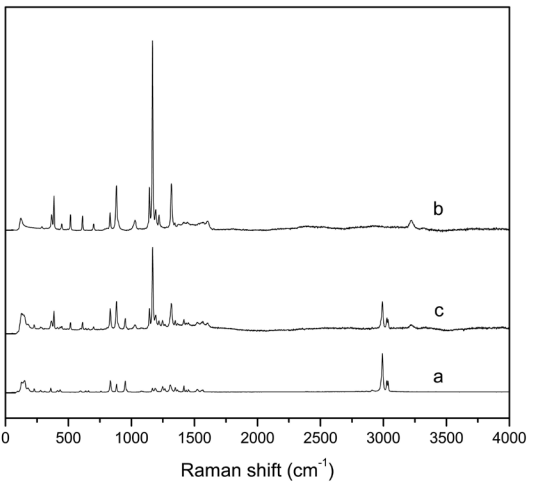

Figure 4. Raman spectra of (a) raw HMX, (b) raw TATB, (c) HMX/TATB co-crystals

Table 1. Assignment of the major bands in the Raman spectra of raw HMX, raw TATB and HMX/TATB co-crystals

Assignments	HMX	Co-crystals	TATB	Assignments
$-CH_2-$ asymmetric stretch	3037.5 3027.8	3214.0 3037.5 3027.8	3223.7	$-NH_2$ stretch
$-CH_2-$ symmetric stretch	2991.7	2993.0 1603.4	1609.0	C−N stretch ($C-NO_2$)
$-NO_2$ asymmetric stretch	1556.2	1565.9		
N−N stretch vibration + $-NO_2$ symmetric stretch	1309.2	1317.2	1317.2	$-NO_2$ symmetric stretch
ring stretch vibration	1189.3	1193.5 1168.5	1167.1	C−N stretch ($C-NH_2$)
ring stretch	950.4	950.4 880.9	880.9	ring stretch

3.5 Mechanical sensitivity

Raw HMX, raw TATB, ultrafine HMX, ultrafine TATB, raw HMX/TATB mixture with a molar ratio of 8/1, ultrafine HMX/TATB mixture with a molar ratio of 8/1 and ultrafine HMX/TATB co-crystals were subjected to impact and friction sensitivity tests, and the results are provided in Table 2. Table 2 shows that reducing the size of the HMX particles and mixing with TATB can reduce the mechanical sensitivity of HMX. The impact and friction sensitivities of ultrafine HMX/TATB explosive co-crystals clearly decreased compared with that of the ultrafine HMX. The drop height of ultrafine explosive co-crystals was increased by 4.8 cm compared with that of the ultrafine HMX/TATB mixture and the explosion probability of friction was 8% lower than that of the ultrafine mixture. These results suggest that the mechanical sensitivity of HMX can be reduced by the formation of co-crystals with TATB. Ultrafine HMX/TATB explosive co-crystals are difficult to initiate under impact and friction conditions and exhibit insensitive characteristics. In addition to the reasons for particle size reduction, the low mechanical sensitivity of HMX/TATB explosive co-crystals is due to the increased degree of hydrogen bonding observed in the co-crystal structure [31].

Table 2. Mechanical sensitivity of explosive samples

Sample	H_{50} [cm]	P [%]
Raw HMX	19.6	84
Raw TATB	>100	0
Ultrafine HMX	47.8	60
Ultrafine TATB	>100	0
Raw HMX/TATB mixture	26.1	76
Ultrafine HMX/TATB mixture	55.7	48
Ultrafine HMX/TATB explosive co-crystals	60.5	40

4 Conclusions

Ultrafine explosive co-crystals of HMX/TATB were prepared by ball milling a suspension of HMX and TATB at a molar ratio of 8/1. The HMX/TATB co-crystals were spherical and ranged from 100 nm to 300 nm. The XRD and DSC patterns of the co-crystals revealed that they are not an intimate mixture of HMX/TATB according to the proportions and that they exhibit a new crystal structure. The Raman spectra indicated that the co-crystals were formed by N−O···H hydrogen bonding between $-NO_2$ (HMX) and $-NH_2$ (TATB).

Compared with ultrafine HMX, the impact and friction sensitivity of the ultrafine co-crystals had decreased significantly, the drop height had increased by 26.57%, and the friction probability had reduced by 20%. The ultrafine HMX/TATB explosive co-crystals exhibited insensitive characteristics towards mechanical stimuli.

Acknowledgements
This work was supported by the Graduate Education Innovation Project of Shanxi Province (2016BY119) and the Advantage Disciplines Climbing Plan of Shanxi Province.

References

[1] Guo, C. Y.; Zhang, H. B.; Wang, X. C.; Sun, J. Research Progress of Cocrystal Explosive. *Mater. Rev.* **2012**, *26*(19): 49-53.
[2] Bolton, O.; Matzger, A. J. Improved Stability and Smart-material Functionality Realized in an Energetic Cocrystal. *Angew. Chem. Int. Ed*. **2011**, *50*(38): 8960-8963.
[3] Yang, Z. W.; Zeng, Q.; Zhou, X. Q.; Zhang, Q.; Nie, F. D.; Huang, H.; Li, H. Z. Cocrystal Explosive Hydrate of a Powerful Explosive, HNIW, with Enhanced Safety. *RSC Adv.* **2014**, *4*(110): 65121-65126.
[4] Zhang, C. Y.; Yang, Z. W.; Zhou, X. Q.; Zhang, C. H.; Ma, Y.; Xu, J. J.; Zhang, Q.; Nie, F. D.; Li, H. Z. Evident Hydrogen Bonded Chains Building CL-20-Based Cocrystals. *Cryst. Growth Des.* **2014**, *14*(8): 3923-3928.
[5] Landenberger, K. B.; Matzger, A. J. Cocrystals of 1,3,5,7-Tetranitro-1,3,5,7-tetrazacyclooctane (HMX). *Cryst. Growth Des.* **2012**, *12*(7): 3603-3609.
[6] Bolton, O.; Simke, L. R.; Pagoria, P. F.; Matzger, A. J. High Power Explosive with Good Sensitivity: a 2 : 1 Cocrystal of CL-20 : HMX. *Cryst. Growth Des.* **2012**, *12*(9): 4311-4314.
[7] Anderson, S. R.; am Ende, D. J.; Salan, J. S.; Samuels, P. Preparation of an Energetic-Energetic Cocrystal Using Resonant Acoustic Mixing. *Propellants Explos. Pyrotech.* **2014**, *39*(5): 637-640.
[8] Landenberger, K. B.; Matzger, A. J. Cocrystal Engineering of a Prototype Energetic Material: Supramolecular Chemistry of 2,4,6-Trinitrotoluene. *Cryst. Growth Des.* **2010**, *10*(12): 5341-5347.
[9] Yang, Z. W.; Li, H. Z.; Zhou, X. Q.; Zhang, C. Y.; Huang, H.; Li, J. S.; Nie, F. D. Characterization and Properties of a Novel Energetic-Energetic Cocrystal Explosive Composed of HNIW and BTF. *Cryst. Growth Des.* **2012**, *12*(11): 5155-5158.
[10] Zhang, H. B.; Guo, C. Y.; Wang, X. C.; Xu, J. J.; He, X.; Liu, Y.; Liu, X. F.; Huang, H.; Sun, J. Five Energetic Cocrystals of BTF by Intermolecular Hydrogen Bond and π-Stacking Interactions. *Cryst. Growth Des.* **2013**, *13*(2): 679-687.

[11] Wu, J. T.; Zhang, J. G.; Li, T.; Li, Z. M.; Zhang, T. L. A Novel Cocrystal Explosive NTO/TZTN with Good Comprehensive Properties. *RSC Adv.* **2015**, *5*(36): 28354-28359.
[12] Wei, C. X.; Duan, X. H.; Liu, C. J.; Liu, Y. G.; Li, J. S. Molecular Simulation on Co-crystal Structure of HMX/TATB. *Acta Chim. Sin.* **2009**, *67*(24): 2822-2826.
[13] Wei, C. X.; Huang, H.; Duan, X. H.; Pei, C. H. Structures and Properties Prediction of HMX/TATB Co-crystal. *Propellants Explos. Pyrotech.* **2011**, *36*(5): 416-423.
[14] Shen, J. P.; Duan, X. H.; Luo, Q. P.; Zhou, Y.; Bao, Q. L.; Ma, Y. J.; Pei, C. H. Preparation and Characterization of a Novel Cocrystal Explosive. *Cryst. Growth Des.* **2011**, *11*(5): 1759-1765.
[15] Song, X. L.; Wang, Y.; An, C. W.; Guo, X. D.; Li, F. S. Dependence of Particle Morphology and Size on the Mechanical Sensitivity and Thermal Stability of Octahydro-1,3,5,7-tetranitro-1,3,5,7-tetrazocine. *J. Hazard. Mater*. **2008**, *159*(2-3): 222-229.
[16] Shi, X. F.; Wang, J. Y.; Li, X. D.; An, C. W. Preparation and Characterization of HMX/Estane Nanocomposites. *Cent. Eur. J. Energ. Mater*. **2014**, *11*(3): 433-442.
[17] Shi, X. F.; Wang, C. L.; Wang, J. Y.; Li, X. D.; An, C. W.; Wang, J.; Ji, W. Process Optimization and Characterization of an HMX/Viton Nanocomposite. *Cent. Eur. J. Energ. Mater.* **2015**, *12*(3): 487-495.
[18] Zohari, N.; Keshavarz, M. H.; Seyedsadjadi, S. A. The Advantages and Shortcomings of Using Nano-sized Energetic Materials. *Cent. Eur. J. Energ. Mater.* **2013**, *10*(1):135-147.
[19] Naya, T.; Kohga, M. Influences of Particle Size and Content of HMX on Burning Characteristics of HMX-Based Propellants. *Aerosp. Sci. Technol*. **2013**, *27*(1): 209-215.
[20] Naya, T.; Kohga, M. Influences of Particle Size and Content of RDX on Burning Characteristics of RDX-based Propellants. *Aerosp. Sci. Technol*. **2014**, *32*(1): 26-34.
[21] Spitzer, D.; Risse, B.; Schnell, F.; Schaefer, M. R. Continuous Engineering of Nano-cocrystals for Medical and Energetic Applications. *Sci. Rep.* **2014**, *4*: 6575.
[22] Doblas, D.; Rosenthal, M.; Burghammer, M.; Chernyshov, D.; Spitzer, D.; Ivanov, D. A. Smart Energetic Nanosized Co-crystals: Exploring Fast Structure Formation and Decomposition. *Cryst. Growth Des.* **2016**, *16*(1): 432-439.
[23] Gao, B.; Wang, D. J.; Zhang, J.; Hu, Y. J.; Shen, J. P.; Wang, J.; Huang, B.; Qiao, Z. Q.; Huang, H.; Nie, F. D.; Yang, G. C. Facile, Continuous and Large-Scale Synthesis of CL-20/HMX Nano Co-crystals with High-Performance by Ultrasonic Spray-assisted Electrostatic Adsorption Method. *J. Mater. Chem. A* **2014**, *2*(47): 19969-19974.
[24] Wang, J. Y.; Li, H. Q.; An, C. W.; Guo, W. J. Preparation and Characterization of Ultrafine CL-20/TNT Cocrystal Explosive by Spray Drying Method. *Chin. J. Energ. Mater*. **2015**, *23*(11): 1103-1106.
[25] Li, H. Q.; An, C. W.; Guo, W. J.; Geng, X. H.; Wang, J. Y.; Xu, W. Z. Preparation and Performance of Nano HMX/TNT Cocrystals. *Propellants Explos. Pyrotech*. **2015**, *40*(5): 652-658.

[26] Majumder, M.; Buckton, G.; Rawlinson-Malone, C.; Williams, A. C.; Spillman, M. J.; Shankland, N.; Shankland, K. A Carbamazepine-indomethacin (1:1) Cocrystal Produced by Milling. *Cryst. Eng. Comm*. **2011**, *13*(21): 6327-6328.
[27] Tan, D.; Loots, L.; Friščić, T. Towards Medicinal Mechanochemistry: Evolution of Milling from Pharmaceutical Solid Form Screening to the Synthesis of Active Pharmaceutical Ingredients (APIs). *Chem. Comm*. **2016**, *52*(50): 7760-7781.
[28] Wang, Y.; Jiang, W.; Song, X. L.; Deng, G. D.; Li, F. S. Insensitive HMX (Octahydro-1,3,5,7-tetranitro-1,3,5,7-tetrazocine) Nanocrystals Fabricated by High-yield, Low-cost Mechanical Milling. *Cent. Eur. J. Energ. Mater.* **2013**, *10*(2): 277-287.
[29] Qiu, H. W.; Patel, R. B.; Damavarapu, R. S.; Stepanov, V. Nanoscale 2CL-20·HMX High Explosive Cocrystal Synthesized by Bead Milling. *Cryst. Eng. Comm.* **2015**, *17*(22): 4080-4083.
[30] *Experimental Methods of Sensitivity and Safety* (in Chinese), National Military Standard of China, GJB/772A-97, **1997**.
[31] Gilardi, R. D.; Butcher, R. J. 2, 6-Diamino-3,5-dinitro-1,4-pyrazine 1-oxide. *Acta Crystallogr. E* **2001**, *57*(7): 657-658.